Accepted for publication in ApJL

Millimeter observations of obscured Spitzer 24 micron sources

D. Lutz[1], L. Yan [2], L. Armus [2], G. Helou [2], L.J. Tacconi [1], R. Genzel [1], A.J. Baker [3,4]

ABSTRACT

We present MAMBO 1.2mm observations of 40 extragalactic sources from the Spitzer First Look Survey that are bright in the mid-infrared ($S_{24\mu m} > 1$mJy) but optically obscured ($log_{10}(\nu F_\nu(24\mu m)/\nu F_\nu(0.7\mu m)) > 1$). We use these observations to search for cold dust emission, probing the similarity of their spectral energy distributions to star forming infrared galaxies or obscured AGN. The sample as a whole is well detected at mean $S_{1.2mm} = 0.74 \pm 0.09$mJy and $S_{1.2mm}/S_{24\mu m} = 0.15 \pm 0.03$. Seven (three) of the sources are individually detected at $> 3\sigma$ ($> 5\sigma$) levels. Mean millimeter fluxes are higher for sources with the reddest mid-infrared/optical colors. Optically faint but with relatively low mm to mid-infrared ratio, the typical SEDs are inconsistent with redshifted SED shapes of local star-forming infrared galaxies. They also differ from SEDs of typical submillimeter selected galaxies, with the 24μm sources that are individually detected by MAMBO possibly representing intermediate objects. Compared to star-forming galaxies, a stronger but optically obscured mid-infrared component without associated strong far-infrared emission has to be included. This component may be due to luminous optically obscured AGN, which would represent a significant part of the high redshift AGN population.

Subject headings: galaxies: starburst, galaxies: active, infrared: galaxies

[1]Max-Planck-Institut für extraterrestrische Physik, Postfach 1312, 85741 Garching, Germany

lutz@mpe.mpg.de, linda@mpe.mpg.de, genzel@mpe.mpg.de

[2]Spitzer Science Center, California Institute of Technology, 1200 East California Boulevard, MC 220-6, Pasadena, CA 91125

lyan@ipac.caltech.edu, lee@ipac.caltech.edu, gxh@ipac.caltech.edu

[3]Jansky Fellow, National Radio Astronomy Observatory

[4]Department of Astronomy, University of Maryland, College Park, MD 20742-2421

ajb@astro.umd.edu

1. Introduction

Significant progress has been made in the last few years in detecting infrared galaxies at high redshift and characterizing their nature, evolution, and contribution to the cosmic background. ISOCAM has detected at 15 μm a population of $z \lesssim 1$ luminous star–forming galaxies (e.g. Elbaz et al. 2002), still fairly bright in the optical (e.g. Flores et al. 1999). SCUBA and MAMBO surveys of small fields detect a distinct $z \sim 2.5$ population of hyperluminous star–forming and active galaxies (for a review see Blain et al. 2002) that are optically extremely faint (e.g. Ivison et al. 2002; Dannerbauer et al. 2004). Spitzer Space Telescope 24 μm surveys sample the redshifted, rest–frame $6 - 12\,\mu$m strong dust emission from PAH and very small grains in galaxies at $z \sim 1-3$. Therefore, deep mid-IR observations using MIPS on Spitzer offer a new and efficient probe of dusty galaxies at high redshift (e.g. Pérez González et al. 2005). Spitzer 24μm surveys are expected to detect all of the ISOCAM and most of the SCUBA/MAMBO sources, bridge the gap between these two populations in redshift and luminosity, and search for entirely new categories of sources.

The first non–proprietary Spitzer survey is the First Look Survey (FLS), covering 3.7 square degrees in seven bands. More than 18000 sources are detected to the 3σ sensitivity of 110 μJy at 24 μm. Combining deep optical, Spitzer IRAC 8 μm, and MIPS 24 μm data, Yan et al. (2004) have obtained the first characterization of a large sample of 24 μm–selected sources. These sources have colors ranging from those of relatively low–redshift, fairly inactive galaxies to extremely red 24 μm/R and 24 μm/8 μm colors that can only be explained by luminous obscured starbursts or AGN at high redshift. The available color information is not unique for identifying the nature of these objects, however, and the applicability of the local SED templates has to be critically examined. This is particularly true for the rare and extreme 24 μm–selected objects that the FLS sample includes due to its large size. In this letter we report on MAMBO 1.2mm observations of such rare 24μm-bright but optically faint sources, providing a constraint on the cold dust contribution to their spectral energy distributions that is essential for characterizing their nature and their relation to other populations of high–redshift infrared galaxies.

2. Sample and Results

Yan et al. (2004) used Spitzer mid-IR and ground-based optical photometry for a first characterization of 24μm sources from the FLS. We have selected for 1.2mm photometry a subset of bright ($S_{24\mu m}$ >1mJy) sources that are optically faint, as evidenced by a 24μm to optical 'color' $R(24, 0.7) \equiv log_{10}(\nu F_\nu(24\mu m)/\nu F_\nu(0.7\mu m))$ of at least 1 (R>22.5 for $S_{24\mu m}$ =1mJy). We have chosen 39 of the 145 sources meeting these criteria, and added

one with a slightly lower R(24,0.7). We refer to these sources as 'obscured 24μm sources'. The selection covers the full color spread of the Yan et al. (2004) objects (Fig. 1), preferring objects brightest at 24μm, and aiming for a large overlap with FLS objects studied by Spitzer mid-IR spectroscopy (Yan et al. 2005, and in preparation). Objects were selected using the Yan et al. (2004) flux catalogs. Since then, slightly revised 24μm and 8μm fluxes (M. Lacy et al. in preparation) have become available which we adopt in the following discussion.

Observations were spread over the pool observing sessions at the IRAM 30m telescope in fall/winter 2004/2005, using the 117 element version of the Max Planck Millimeter Bolometer (MAMBO) array (Kreysa et al. 1998) operating at a wavelength of 1.2mm. On-off observations were typically obtained in blocks of 6 scans of 20 subscans each, and repeated in later observing nights until reaching noise near 0.66mJy or a 5σ detection. The median 1.2mm noise level reached for the sample is 0.59mJy (range 0.35 to 0.82mJy). The data were reduced with standard procedures in the MOPSIC package developed by R. Zylka, using the default calibration files for these two pool periods. Table 1 lists the resulting 1.2mm fluxes and their statistical uncertainties.

Three sources are detected individually at more than 5σ with 1.2mm fluxes between 2.3 and 5.8mJy, and four more at 3σ to 5σ. The total 40 object sample is well detected statistically at a mean flux of 0.74$\pm$0.09mJy (Table 2). To investigate a dependence on the mid-IR/optical colors, we have grouped the sample in four color 'quadrants' separated at R(24,0.7)=1.5 and and R(24,8)=0.5. Due to the sample selection, these quadrants contain similar numbers of objects by design. Table 2 shows clear trends in the mean 1.2mm fluxes for these subsamples. Objects redder in R(24,0.7) have significantly higher mean 1.2mm flux, and a trend may also be present with R(24,8). Values quoted in Table 2 refer to means of the individual source data weighted by the inverse of the noise squared. Very similar values are obtained for equal weight means. The trend in the mean fluxes agrees with the $> 3\sigma$ detection of 7/24 objects at R(24,0.7)>1.5 vs. 0/16 at bluer color. Using the formalism of Stevens et al. (2005), this implies that the two groups are different at 2.9σ significance. The distribution of 1.2mm vs. 24μm fluxes, shown in Fig. 2, is inconsistent with a single flux ratio for the entire sample, or for the subsample with R(24,0.7)>1.5. This is expected given the sample selection, and emphasizes that the mean values quoted in Table 2 are formed over (sub)samples that can have noticeable spreads of intrinsic properties.

3. Millimeter properties of obscured Spitzer sources

Our color selection implies that these objects must be heavily obscured and/or at considerable redshift. This is illustrated in Fig. 3, showing that even spectral energy distribu-

tions similar to 'standard' dusty starbursts like M82 fail to reproduce for plausible redshifts R(24,0.7)>1.2, i.e. the vast majority of our sample. R(24,0.7) will be yet lower for SEDs of UV-brighter starbursts like NGC 7714. SEDs similar to the most optically obscured local ultraluminous infrared galaxies like Arp220 reach R(24,0.7)>1.5 for redshifts around 2, but even stronger emission at observed 24μm (rest-frame 8μm for z$\approx$2) relative to the shorter wavelengths is needed to reproduce the most extreme Spitzer objects. The same is true for the SED of the well studied less luminous but extremely obscured galaxy, NGC 4418. For this object, both the 8μm and the 0.7μm flux are host dominated at z$\gtrsim$1.5. Varying the nucleus to host ratio moves the source diagonally in Fig. 3.

The millimeter observations provide a crucial test of the analogy to local SEDs. Fig. 4 shows the expected ratio of 1.2mm and 24μm flux density as a function of redshift, again for M82, Arp220, and NGC 4418 SEDs. The seven objects with individual MAMBO detections are reasonably close to the properties of these local templates. At $S_{1.2mm}/S_{24\mu m} \sim 1 \ldots 5$, they are in a range still consistent with local infrared galaxy SEDs redshifted to z$\sim$2, assuming a relatively high optical obscuration or modest additional mid-iR emission. In contrast, comparison of the templates to the mean values for the obscured Spitzer sources (Table 2) shows that in fact neither SED provides a good representation of the mean properties of our 24μm sources. Arp 220 and NGC 4418–like SEDs, which were in a reasonable range of the optical/mid-IR colors, predict by far too strong 1.2mm flux for plausible redshifts. M82-like SEDs are closer to the observed mm to MIR ratio, but predict too bright optical counterparts as noted above. We conclude from the analysis of mean properties that the sample of obscured 24μm contains many sources that are not well fit by these local infrared luminous galaxy SED templates. Relative to the templates, they require additional rest frame mid-IR emission, due to a component that is both warm (to avoid overproducing mm emission) and optically obscured.

Another way of phrasing the need for 'additional rest frame mid-IR emission' is to state that the overall infrared SED must be warm to hot, without a dominant rest frame far-IR peak. In a strongly simplifying single temperature blackbody fit, the observed 1.2mm to 24μm flux density ratio corresponds to a temperature of $\sim$75K, i.e. intrinsic T$\gtrsim$200K if at z$\sim$2, and luminosities of the order of $10^{13} L_{\odot}$. The warm temperature is suggestive of a strong AGN contribution. The SED of the most luminous radio-quiet local quasar, PDS 456 (Yun et al. 2004) is able to fit the 1.2mm/24μm ratio for plausible redshifts (Fig. 4), but this Type 1 object is too bright in the UV/optical to explain the mid-IR/optical colors for our sample. That more obscured AGN may be able to meet that constraint can be illustrated using the *nuclear* SED of the classical Seyfert 2 NGC 1068. Its nuclear FIR/submm emission can currently be separated from the host only at 450μm with $S_{450\mu m} \sim 1.5$Jy (Papadopoulos & Seaquist 1999), but this can be combined with the mid-IR AGN continuum (Lutz et al. 2000)

and the rest frame UV taken from NED, to conclude that such an AGN SED would satisfy the criteria for both faintness at 1.2mm (Fig. 4) and optical obscuration (Fig. 1). AGN in obscured 24μm sources must suffer intermediate obscuration, sufficient to suppress the rest frame UV/optical but not moving too much energy into far-IR re-emission. Separation from host emission and spectral characterization of the rest frame far-IR emission is currently incomplete for local obscured AGN, but objects like IRAS F00183-00183 (Tran et al. 2001; Spoon et al. 2004) do have more favourable mid- to far-IR ratios than NGC 4418 and may fit the SEDs of some obscured 24μm sources.

Low 1.2mm/24μm flux ratios can also be obtained for low redshift ($z \lesssim 1$) infrared star-forming galaxy SEDs. As already noted, this is ruled out for the adopted templates, by the failure to meet R(24,0.7)>1 at such redshifts (Fig. 3). Contamination by similar sources may occur at the low R(24,0.7) end of the MAMBO sample if the scatter in rest frame SEDs extends towards smaller optical/mid-IR flux ratios. This scenario becomes progressively unlikely for the R(24,0.7)>1.5 sources with weak 1.2mm emission.

Hunt et al. (2005) use the likely compactness of star formation events in high redshift infrared galaxies to argue for SEDs of Blue Compact Dwarf Galaxies as local analogues. The most extreme case, SBS 0335-052, shows an absorbed warm mid-IR continuum (Thuan et al. 1999; Houck et al. 2004). While this possible analogy has to be mentioned, it is unclear to which extent such low metallicity dwarfs can relate to the luminous obscured 24μm sources. SBS 0335-052, in addition to its mid-IR emission, has strong unobscured optical/UV emission which would place it far off the color selection of obscured 24μm sources. Rest frame submm information is not available to place SBS 0335-052 on Fig. 4.

4. Relation to other populations

(Sub)millimeter galaxies (SMGs) are the best studied pre-Spitzer population of z> 1.5 infrared galaxies, inferred to be objects at z$\sim$2.5 with roughly ULIRG like SEDs but much higher luminosity. Optical to mid-IR colors of bright and obscured 24μm sources (Figs. 1,3) and their low surface density compared to that of SMGs could have been consistent with an identification of the yet more extreme luminosity end of the SMG population as obscured 24μm sources. The small ratio of 1.2mm and 24μm emission clearly argues against this being true for the majority of the Spitzer sources. Egami et al. (2004), Ivison et al. (2004), and Frayer et al. (2004) have reported 24μm photometry of SMGs from SCUBA and MAMBO blank field and radio preselected surveys. They find much higher $S_{1.2mm}/S_{24\mu m}$, with median $\sim$ 12, clearly inconsistent with SMGs' and obscured Spitzer sources' having similar SED shapes and redshifts. Again, the Spitzer objects with individual MAMBO detections are

closer to the SMG properties.

Blain et al. (2004) discuss selection effects against warm SEDs in the SMG population and the potential of Spitzer in avoiding them. In a related effort, Chapman et al. (2004) have obtained spectroscopic redshifts of optically faint μJy radio sources without submm detections, inferring under the assumption of the radio – far-IR correlation that these must represent a population of ultraluminous star-forming z$\sim$2.2 galaxies characterized by intrinsically warm or hot dust continua. Little is known at present about the rest-frame mid-IR properties of these sources, making an assessment of the overlap with obscured 24μm sources difficult. Frayer et al. (2004) report faint 24μm fluxes or nondetections of several optically faint radio sources that have SCUBA 850μm flux upper limits of order 8mJy. If these results are representative for the full population of optically faint radio sources, then their possible warm FIR SEDs cannot extend down into the mid-IR, and their nature must be different from the obscured 24μm sources. If, for example, their radio emission is AGN boosted, their dust emission may be comparatively weak at all wavelengths.

Mid-IR spectroscopy will play a key role in identifying the nature of the rare obscured 24μm sources and their strong mid-IR emission. Houck et al. (2005) and Yan et al. (2005) have reported the first Spitzer IRS spectroscopy of such sources, finding a predominance of continua and absorbed continua and indications for starburst PAH emission in a subset of sources. The obscured continuum spectra, which are seen only in a small minority of local infrared galaxies (Spoon et al. 2002) but a third to half of the obscured 24μm sources in the subsamples already published by Houck et al. (2005) and Yan et al. (2005), indicate heavily embedded energy sources that might be AGN. Redshift estimates, where they can be derived, suggest z$\sim$1.5–3. As for the photometric evidence, comparison to initial Spitzer spectroscopy of SMGs which shows PAHs (Lutz et al. 2005) suggests that the two populations have only modest overlap, and that there is a large contribution of warm and possibly AGN like sources to the obscured 24μm population.

If a good part of the bright obscured 24μm sources contain luminous high z AGN they will represent a significant component of the high redshift AGN population. Our MAMBO sample is a subset of about 150 similar objects (Fig. 1) detected over the 3.7 square degree FLS field. If many of these objects are $L_{Bol} \sim 10^{13}$L$_\odot$ AGN at z$\sim$1.5-3 their comoving number density will be of the order 10^{-6}Mpc^{-3}, comparable to that of similar bolometric luminosity (M$_B < -25$) optically selected quasars (Croom et al. 2004). The ongoing characterization of their redshift distribution and SEDs will shed more light on this issue.

Based on observations carried out with the IRAM 30m telescope and with the Spitzer Space Telescope. We thank the IRAM staff for support and advice, all pool observers for

their help in obtaining the observations, and the referee for helpful comments.

REFERENCES

Blain, A.W., Smail, I., Ivison, R.J., Kneib, J.-P., Frayer, D.T., 2002, PhR, 369, 111

Blain, A.W., Chapman, S.C., Smail, I., Ivison, R. 2004, ApJ, 611, 52

Chapman, S.C., Smail, I., Blain, A.W., Ivison, R.J. 2004, ApJ, 614, 671

Croom S.M., Smith, R.J., Boyle, B.J., Shanks, T., Miller, L., Outram, P.J., Loaring, N.S. 2004, MNRAS, 249, 1397

Dannerbauer, H., Lehnert, M.D., Lutz, D., Tacconi, L., Bertoldi, F., Carilli, C., Genzel, R., Menten, K. 2004, ApJ, 606, 664

Egami, E., et al. 2004, ApJS, 154, 130

Elbaz, D., Cesarsky, C.J., Chanial, P., Aussel, H., Franceschini, A., Fadda, D., Chary, R.R. 2002, A&A, 384, 848

Flores, H., et al. 1999, ApJ, 517, 148

Förster Schreiber, N.M., Sauvage, M., Charmandaris, V., Laurent, O., Gallais, P., Mirabel, I.F., Vigroux, L. 2003, A&A, 399, 833

Frayer, D.T., et al. 2004, ApJS, 154, 137

Houck, J., et al. 2004, ApJS, 154, 211

Houck, J., et al. 2005, ApJ, 622, L105

Hunt, L., Maiolino, R. 2005, ApJ, 626, L15

Ivison, R.J., et al. 2002, MNRAS, 337, 1

Ivison, R.J., et al. 2004, ApJS, 154, 124

Kreysa, E. et al. 1998, Proc. SPIE, 3357, 319

Lutz, D., Sturm, E., Genzel, R., Moorwood, A.F.M., Alexander, T., Netzer, H., Sternberg, A. 2000, ApJ, 536, 697

Lutz, D., Valiante, E., Sturm, E., Genzel, R., Tacconi, L.J., Lehnert, M.D., Sternberg, A., Baker, A.J. 2005, ApJ, 625, L83

Papadopoulos, P.P., Seaquist, E.R. 1999, ApJ, 514, L95

Pérez González, P.G., et al. 2005, ApJ, in press (astro-ph/0505101)

Roche, P.F., Aitken, D.K., Smith, C.H., James, S.D. 1986, MNRAS, 218, 19p

Spoon, H.W.W., Keane, J.V., Tielens, A.G.G.M., Lutz, D., Moorwood, A.F.M. 2001, A&A, 365, L353

Spoon, H.W.W., et al. 2002, A&A, 385, 1022

Spoon, H.W.W., et al. 2004, ApJS, 154, 184

Stevens, J.A., Page, M.J., Ivison, R.J., Carrera, F.J., Mittaz, J.P.D., Smail, I., McHardy, I.M. 2005 MNRAS, 360, 610

Thuan, T.X., Sauvage, M., Madden, S. 1999, ApJ, 516, 783

Tran, Q.D., et al. 2001, ApJ, 552, 527

Yan, L., et al. 2004, ApJS, 154, 60

Yan, L., et al. 2005, ApJ, 628, 604

Yun, M.S., Reddy, N.A., Scoville, N.Z., Frayer, D.T., Robson, E.I., Tilanus, R.P.J. 2004, ApJ, 601, 723

Table 1. MAMBO 1.2mm fluxes of obscured 24μm sources

ID	RA J2000	DEC J2000	$S_{1.2mm}$ mJy	$S_{24\mu m}$ mJy
39	17:17:50.65	58:47:45.1	-0.14±0.65	5.04
42	17:17:58.44	59:28:16.8	0.43±0.62	4.93
45	17:11:47.46	58:58:40.0	0.16±0.65	4.75
78	17:15:38.18	59:25:40.1	-0.25±0.62	3.11
110	17:12:15.44	58:52:27.9	-0.42±0.55	2.40
133	17:14:33.68	59:21:19.3	0.01±0.57	2.08
180	17:15:43.54	58:35:31.2	1.26±0.44	1.76
227	17:14:56.24	58:38:16.2	-0.41±0.58	1.55
289	17:13:50.00	58:56:56.8	2.28±0.35	1.34
464	17:14:39.57	58:56:32.1	-0.27±0.65	1.00
7967	17:18:31.68	59:53:17.2	0.22±0.51	8.04
7977	17:14:19.96	60:27:24.8	-1.18±0.63	5.78
8034	17:12:10.28	60:18:58.1	0.74±0.62	3.04
8069	17:15:00.36	59:56:11.5	0.21±0.63	2.51
8107	17:16:38.65	59:49:44.4	0.70±0.60	2.01
8135	17:14:55.71	60:08:22.6	3.49±0.49	1.85
8182	17:14:34.56	60:28:28.7	1.87±0.50	1.61
8184	17:12:26.76	59:59:53.5	0.72±0.62	1.61
8185	17:14:22.85	60:28:34.7	0.20±0.62	1.61
8196	17:15:10.28	60:09:55.2	0.99±0.43	1.57
8245	17:15:36.34	59:36:14.8	-0.49±0.46	1.41
8268	17:16:24.74	59:37:52.6	-0.45±0.78	1.31
8377	17:17:33.51	59:46:40.4	0.72±0.57	1.09
15690	17:19:22.44	60:14:56.2	0.89±0.52	5.44
15776	17:20:50.66	59:32:54.2	0.81±0.54	2.30
15840	17:19:22.40	60:05:00.3	-0.08±0.57	1.90
15880	17:21:19.46	59:58:17.2	2.06±0.53	1.68
15890	17:24:48.65	60:14:39.1	0.65±0.67	1.64
15929	17:24:06.95	59:24:16.3	0.54±0.56	1.51
15943	17:20:18.06	59:29:01.2	0.14±0.55	1.46

Table 1—Continued

ID	RA J2000	DEC J2000	$S_{1.2mm}$ mJy	$S_{24\mu m}$ mJy
15972	17:25:29.32	59:57:30.7	0.02±0.63	1.37
16030	17:20:00.32	60:15:20.9	0.09±0.69	1.25
22195	17:20:44.81	58:29:23.7	-0.19±0.69	5.05
22204	17:18:44.38	59:20:00.5	0.27±0.51	4.29
22303	17:18:48.80	58:51:15.1	-1.05±0.64	2.12
22314	17:19:27.28	59:15:36.3	1.70±0.55	2.02
22397	17:20:05.96	59:17:45.0	0.39±0.72	1.59
22404	17:21:51.77	58:53:27.7	0.66±0.59	1.57
22563	17:22:49.00	58:50:27.5	5.79±0.82	1.14
22582	17:21:24.58	59:20:29.5	2.22±0.53	1.11

Table 2. Mean 1.2mm properties for different ranges of mid-IR/optical colors

R(24,0.7)	R(24,8)	N	$\sigma_{1.2}$ mJy	$S_{1.2mm}$ mJy	$S_{1.2mm}/S_{24\mu m}$
all	all	40	0.59	0.74±0.09	0.15±0.03
<1.5	<0.5	8	0.65	0.15±0.22	0.01±0.05
<1.5	≥0.5	8	0.59	0.46±0.20	0.26±0.11
≥1.5	<0.5	15	0.57	0.91±0.14	0.18±0.05
≥1.5	≥0.5	9	0.53	1.08±0.18	0.52±0.10

Note. — See Fig. 1 for the distribution of sources within the R(24,0.7) and R(24,8) colors. $\sigma_{1.2}$ indicates the median 1.2mm flux error for the sources in each bin.

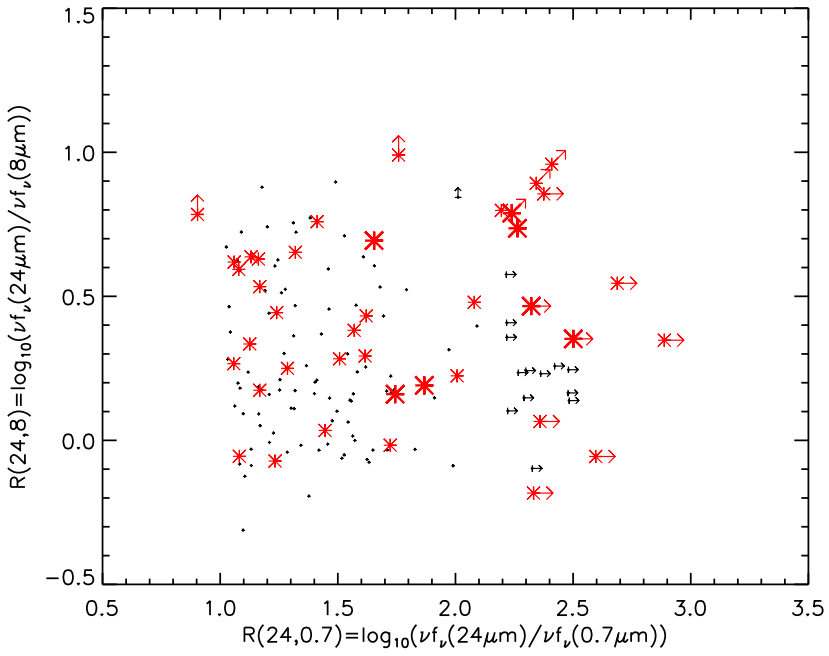

Fig. 1.— Optical/mid-IR color-color plot of bright (>1mJy) 24μm sources from the Yan et al. (2004) Spitzer FLS sample, indicated by small crosses. Sources with R(24,0.7)<1 are not shown. Asterisks highlight the targets observed by MAMBO, big asterisks those individually detected by MAMBO at the $\geq 3\sigma$ level. 8μm and optical limits are 3σ.

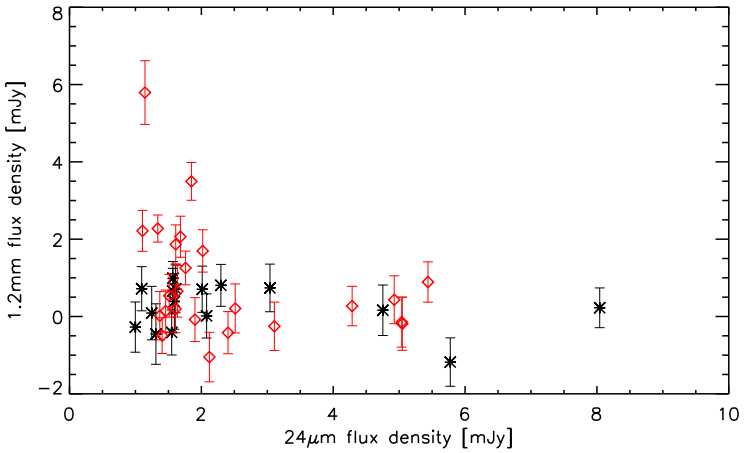

Fig. 2.— MAMBO 1.2mm fluxes as a function of 24μm fluxes. 24μm errors are smaller than the symbols. Sources with R(24,0.7)>1.5 are shown as diamonds, others as asterisks.

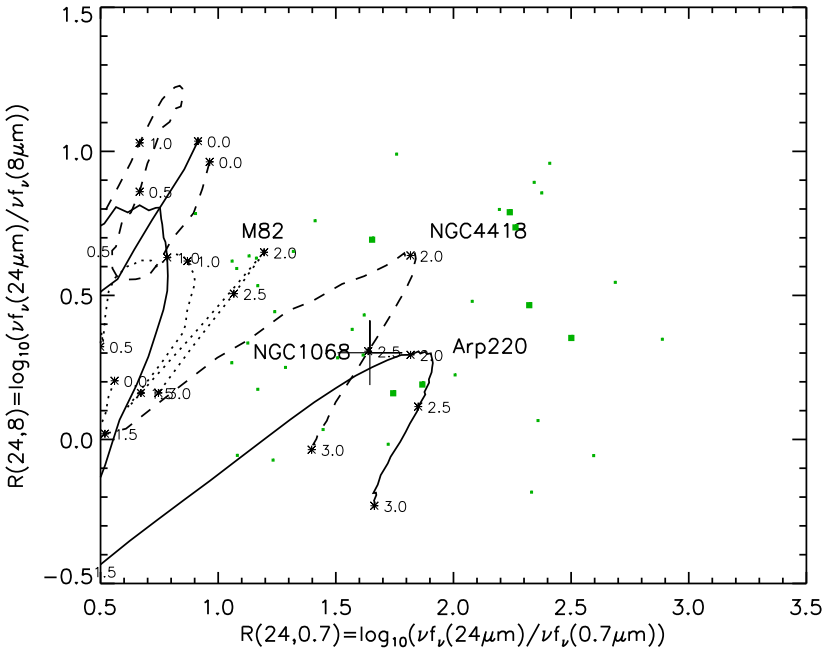

Fig. 3.— Mid-IR/optical colors for redshifted objects with the SEDs of the star forming infrared galaxies M82 and Arp220, and of the heavily obscured galaxy NGC 4418. Locations of the FLS sources observed by MAMBO are repeated from Fig. 1. Redshifts from 0 to 3 are marked in intervals of 0.5. The adopted SEDs are based on observations for large apertures taken from the literature. The key rest frame mid-IR range uses the ISOCAM-CVF low resolution spectra of Förster Schreiber et al. (2003) for M82, O. Laurent (priv. comm) for Arp 220, and ISOPHOT-S (Spoon et al. 2001) and groundbased spectra (Roche et al. 1986) for NGC 4418. The colors of the nuclear region of the Type 2 AGN NGC 1068 shifted to z∼1.67 are indicated by a cross.

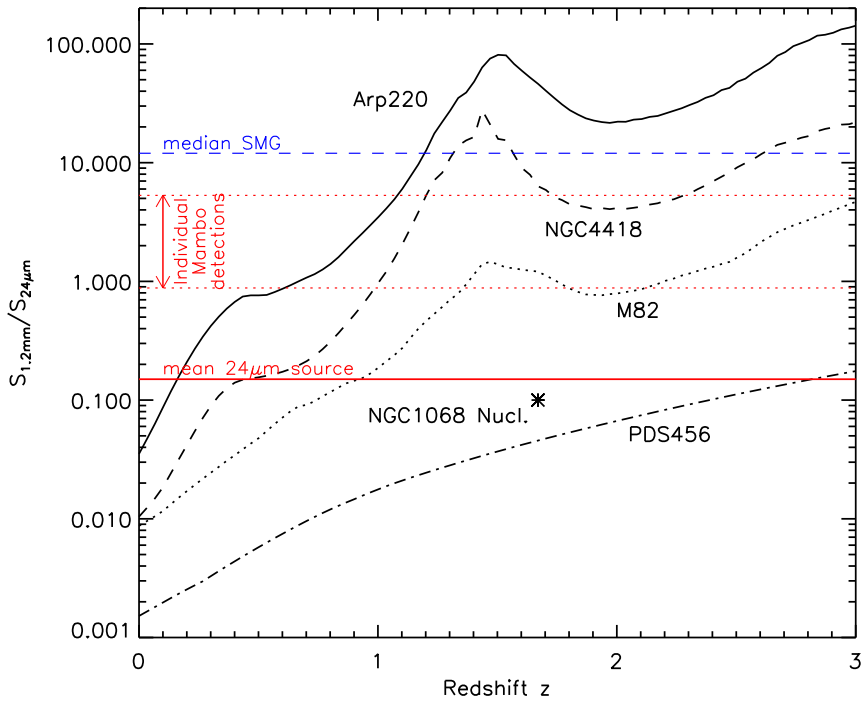

Fig. 4.— Ratio of 1.2mm and 24μm flux density as a function of redshift for local SED templates. The SEDs of M82 and Arp220 represent typical and extremely obscured star-forming infrared galaxies. NGC 4418 is an extremely obscured compact object possibly hosting an AGN. PDS456 is a luminous quasar whose infrared SED is dominated by the AGN mid-IR emission, with a weak far-IR component. The AGN dominated nuclear region of NGC 1068 is only shown for a single redshift where the rest frame submm emission of the nucleus can be spatially isolated. The horizontal continuous line shows the mean ratio for our sample. Horizontal dotted lines indicate the range spanned by the targets that are individually detected by MAMBO. The horizontal dashed line indicates the median 1.2mm to 24μm flux ratio for submillimeter galaxies (SMGs) – see text for references.